Energies **2015**, *8*, 2358-2380; doi:10.3390/en8042358

OPEN ACCESS

energies

ISSN 1996-1073

www.mdpi.com/journal/energies

Article

Design and Energy Performance of a Buoyancy Driven Exterior Shading Device for Building Application in Taiwan

Kuo-Tsang Huang [1], Kevin Fong-Rey Liu [2] and Han-Hsi Liang [3,*]

[1] Department of Bioenvironmental Systems Engineering, National Taiwan University, No. 1, Sec. 4, Roosevelt Rd., Taipei 10617, Taiwan; E-Mail: huangkt@ntu.edu.tw

[2] Department of Safety, Health and Environmental Engineering, Ming Chi University of Technology, No. 84 Gungjuan Rd., Taishan District, New Taipei City 24301, Taiwan; E-Mail: kevinliu@mail.mcut.edu.tw

[3] Department of Architecture, National United University, No. 1, Lien-Da, Miaoli 36003, Taiwan

* Author to whom correspondence should be addressed; E-Mail: lhh@nuu.edu.tw; Tel.: +886-37-381-635; Fax: +886-37-354-838.

Academic Editor: Hossam A. Gabbar

Received: 15 January 2015 / Accepted: 16 March 2015 / Published: 25 March 2015

Abstract: Traditional dynamic shading systems are usually driven by electricity for continuously controlling the angle of blind slats to minimize the indoor solar heat gain over times. This paper proposed a novel design of buoyancy driven dynamic shading system, using only minimum amount of electricity. The energy performance and the improved thermal comfort induced by the system were simulated by EnergyPlus for a typical office space under the context of Taiwanese climate. The design processes are composed of three parts: an alterable angle of blind slats that raises the energy performance to be suitable for every orientation, the buoyancy driven transmission mechanism, and a humanized controller that ensures its convenience. The environmental friendly design aspects and control mechanisms to fulfill demands for manufacturing, assembling, maintenance and recycling, *etc.*, were also presented as readily for building application. Besides, the effectiveness of cooling energy saving and thermal comfort enhancing were compared against the cases without exterior blinds and with traditional fixed blinds installed. The results show that the cooling energy is drastically reduced over times and the blind system is effectively enhancing the indoor thermal comfort.

Keywords: dynamic shading device; buoyancy driven; energy saving; thermal comfort

1. Introduction

Energy saving methods for technical design in buildings are more and more widely used. For instance, the use of shading devices has led to practical applications for improving energy performance. Shading and daylight should always be optimized in order to consider both the energy-saving and environmental aspects of design. This design paradigm accounts for current trends in the design of buildings, especially school buildings that have large glazing areas and superior shading devices. It is evident that the design issues concerning overheating and cooling demand have also become important considerations.

A shading device operates to decrease solar heat gain so that total heat flow is not only delayed, but also actually reduced. The solar gain constitutes a major portion of the air-conditioning load around the perimeter zone of a building in hot and humid areas. Statistics showed that in Taiwan, more than 30% of all electrical power was consumed by air-conditioning [1]. Therefore, the use of external shading devices would save 25% of the total consumption of direct air-conditioning power [2]. External shading devices have always been a simple and low-cost device used to control the heating effect of natural light and reduce overall cooling loads. Kim *et al.* [3] proposed an experimental configuration of an external shading device that would result in the most efficient cooling outcomes through adjustments to the slat angle. Passive and adaptive shading device designs can be found in [4]. Yener [5] developed a mathematical model to determine the optimal solution for fixed shading devices. Carbonari *et al.* [6] presented a study on the optimal shading device for the orientation of buildings. Moreover, it was found that 70% of heating gained might be reduced in summer through the installation of fixed horizontal louver shading devices [7]. The external fixed shading device's geometry was optimized in order to reduce the overall energy consumption in an office room with extensive glazing and moveable venetian blinds [8]. Furthermore, Hammad *et al.* [9] explored the influence of external dynamic louvers on the energy consumption of an office building located in Middle East region and identified the optimal angle for louvers with respect to energy performance. Study by Nielsen *et al.* [10] is of a seldom research using purely computer simulation technique in quantifying several physical performance including energy demand, indoor air quality, the amount of daylight available, and visual comfort.

In the past, various studies have suggested that the use of shading devices could represent a way to improve energy consumption and increase user comfort in buildings [3,5,11]. The current challenge is to develop integrated approaches for the implementation and control of such devices [12–14], while considering both visual comfort and energy performance in the design. Most of these tools have been developed to optimize the function of external shading devices from different viewpoints. The features of such methods are related to the complexity of the problem, for instance the stage of building design and the desired accuracy. Buoyancy forces arise as a result of variations of density in a fluid subject to gravity, and produce a wide range of phenomena of importance in many branches of fluid mechanics [15]. Slab buoyancy provides the primary driving force for subduction and slab density plays

an important control factor [16]. Several authors have argued that the material's super-hydrophobic property and high porosity will significantly modulate slab buoyancy [17,18]. This paper presents evidence to suggest that there is a simplified control mechanism that incorporates the automatic buoyancy method in external shading devices equipped with horizontal panels. For instance, a shading device could be installed on the exterior of the building and designed to minimize the radiant heat and maximize illumination. Cheng *et al.* [19] simulated the solar radiation received on various orientations of four major cities from north to south (25–22 °N) in Taiwan. The simulated data indicated that there is lower solar radiation when simulation orientations are in the ENE–WNW and SSE–SSW, compared to the other orientations. The results of that study were adopted as a primary reference for the rotation mechanism of the blind slats within a day. This paper discusses improvements to the proposed external shading device so that a lower price and higher efficiency can be achieved. The purpose of the proposed design is to effectively control the building's interior environment in a manner that is acceptable to the public. A further objective of this paper is to discuss the impacts of energy performance and indoor thermal comfort on the development of an external shading device system. The cooling energy saving and thermal comfort simulation software that is used to analyze a typical office space considers different orientations and climatic zones in Taiwan. The data form the simulations will facilitate the implementation of future applications in order to reduce the overall energy consumption and operational costs of the building [20,21].

2. Design Consideration

In the operation of automatic controllers, buoyancy shading devices do not require logical calculations, although the energy consumption will be lowered. This feature renders the buoyancy-driven system a suitable controller that may replace the traditional power source. In this study, consideration is given to both the direction of the panel and the angle of rotation that is required to fulfill the functional requirements of the design and user's preferences. As far as these criteria are concerned, the design of the shading device is greatly different from that of the existing external shading device, however both the geometry and assembly process have been modified so as to simplify the manufacturing process. The control of the developed shading system doesn't use much of electric device as compared to the other existing kinds, which minimized the electricity need for operation. Furthermore, by referencing the receiving solar radiation to maximize daylighting availability from [19], a quasi-optimized movement mechanism of the blind slats could be obtained. The rotation of the blind slats is commenced by the linking horizontal pivots, which are driven exclusively by buoyancy force. Consequently, the angle of shading and the rotation speed of the slats could be adjustable to meet users' or designers' needs. The design provides an alternative automatic control option of the exterior shading blinds for the application on windows of office spaces or rural houses. This paper explains the method involved in making an efficient controller which operates in real time, reacts properly to different situations, and may be completely controlled by the user. This study expects to become user acceptance data concerning automatic control systems in buildings and bases on the earlier discussion in this report [22].

The design specifications of the shading device are a necessary part of the design's long-term performance. Figure 1 shows the design specifications that were considered during the design process of the shading device and can be summarized as follows:

(1) The application must be realistic and practical.
(2) All details must be improved, especially the design process and generation.
(3) The design may be extensively used.
(4) It must also possess the function of home security.
(5) It must include all facts relevant to product maintenance.
(6) The concepts may be improved in the future.

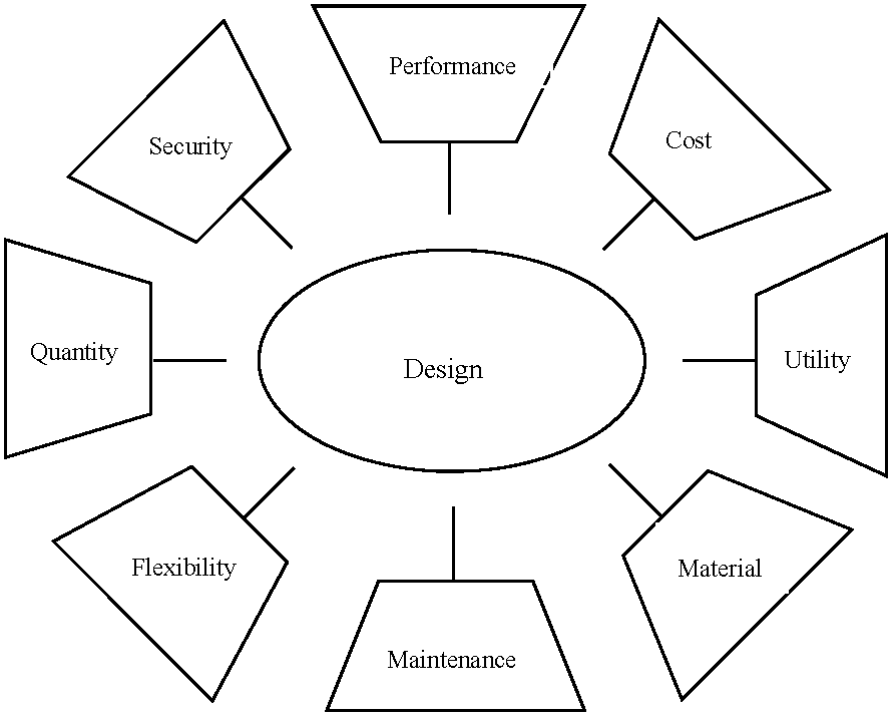

Figure 1. Design specifications of the shading device.

3. Methodology

The entire design process comprised of distinct stages that represented a complete sequence of design activities based on perceived user needs. The configuration of the shading device was the result of various design processes that are shown in Figure 2. This paper details all the activities that were carried out in relation to the design. Overall, the aims is to present the concept of a functional, structural design. Finally, the detailed design of a final product is also presented.

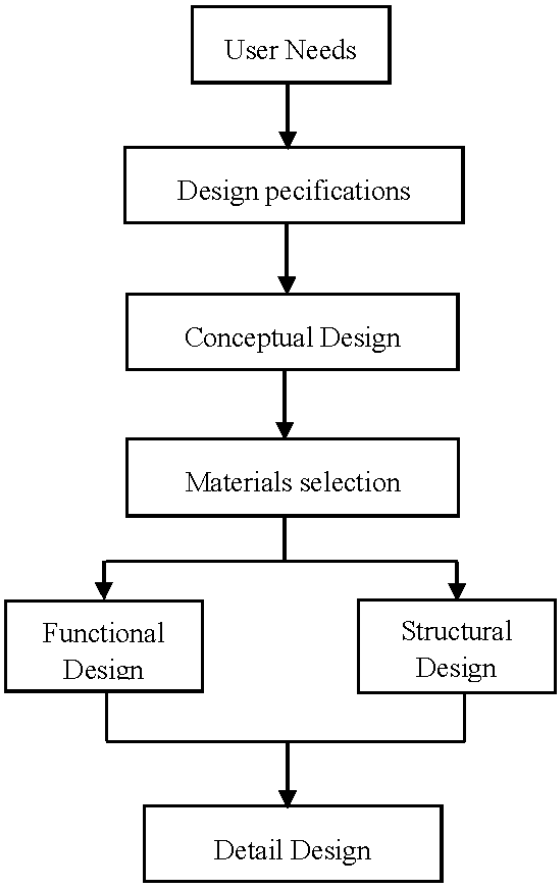

Figure 2. Design processes involved within the shading device.

3.1. Materials Selection

The materials were divided into two types, depending on the part that was used; the selection of materials and each requisite function are shown in Table 1. The materials used for the frame of the proposed design included aluminum alloy and acrylic-plastic. There were four key reasons for the selection of these materials for use in the design:

(1) Security requirement

Security is a major factor to be considered when selecting materials. The strength of the design in this area is important given its, security function; the shading device provides shelter and replaces the traditional method.

(2) Weather resistance

It is difficult to maintain and keep clean when an external shading device is used, especially when it is installed outside the building. However, both weather resistant design and resilient materials can resolve this problem.

(3) Construction

The shading device should be easy to constructed and be tailor-made in accordance with the size of the window. This aspect should not influence the function and quality of design under construction.

(4) Cost-effectiveness and flexibility

Considering user requirements, the proposed device is much more flexible in comparison to a fixed shading device. Due to it cost-effectiveness, the use of the automatic shading device can increase user satisfaction.

Table 1. Summary of materials selection and function.

Diagram		
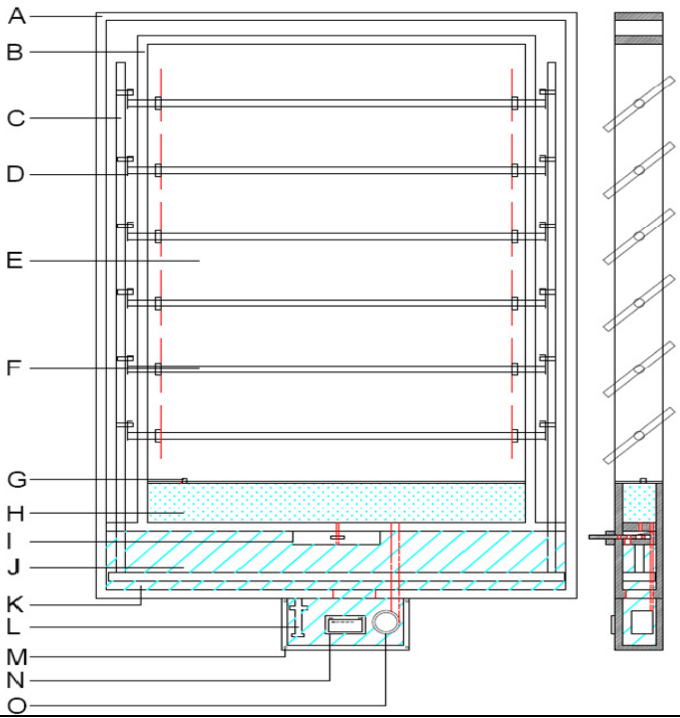		
Position	**Designation**	**Description**
A	External frame	Aluminum alloy, offer frame stability and security function
B	Interior frame	Aluminum alloy, offer frame stability and security function
C	Drive lever	Acrylic-plastic, move upward along with the uplifting level of liquid surface inside the compartment
D	Link	Acrylic-plastic, one end connected to the drive lever and the other, to the pivot
E	Panel	Acrylic-plastic, offer sun-shielding and daylight function
F	Pivot	Aluminum alloy, drive the panel to turn toward the intended direction and offer security function
G	Liquid supply hole	Rubber material, introduce liquid into the system
H	Upper chamber	Propose using liquid, provide the liquid volume required to turn the sun shading panel just for 60°
I	Liquid compartment	Connect to upper and lower chambers
J	Floating board	Expandable-polystyrene, offer the upward force and make drive lever rise, super-hydrophobic and high porosity
K	Lower chamber	Install floating board and make it move upward along with the uplifting level of liquid surface
L	Liquid level controller	Control the suitable time and pumping volume of motor
M	Maintenance section	Battery Replacement and motor maintenance
N	On-off switch	Set the operation time and the start switch
O	Motor	Convey the liquid of lower chamber to the upper one

3.2. Functional and Structural Design

Good shading device settings would adjust the design of form to adapt to facade orientation and opening shape. However, it is also important to consider other conditions, such as daylighting and ventilation. According to the above description and the simulated results [19], the rotation mechanism of the slats in facing various orientations to consider both for minimizing solar heat gain and maximizing daylighting and ventilation. The panel would be installed into two driving and rotating mechanisms to match up two types of the location of the building. Using the control mechanism of buoyancy, the panel could be adjusted to face the sun representing the most suitable real-time operation that can be used to satisfy user demand. Moreover, this design considers the correlation between the driving mechanism and water level control of buoyancy and includes an analysis of the components of the linkage design. The most essential design function relates to the rotating panels, in particular how they could be installed in relation to the location of windows. Figure 3 shows the driving and rotating mechanisms of panels in different directions. In Taiwan, it is a design convention for alloy bars to be added to the external walls across windows as a means of increasing security (Figure 4). For this configuration, a different rotation system and metal frame structure was required. In fact, because it supported the rotating mechanism, the outline frame and rotating members were the most critical structural part of the new external shading device. Figure 5 shows the details of the major parts of the configuration and the frame that was designed to hold the shading device.

The external shading device comprises of three parts: the outline frame, drive device and floating-provided liquid compartment. The frame is equipped with sun shading panels that turn with the upward force of the floating boards and provide the appropriate amount of shade according to different sunshine angles. One end of the drive device is located inside the liquid compartment, with the other end connecting to the panel through a link, which moves upward along with the increasing level of liquid surface, thus, the sun-shading panel is forced to turn when the sun-shielding angle is required to be changed. The liquid compartment consists of two interlinked upper and lower chambers and the liquid is allowed to flow within the upper and lower chambers.

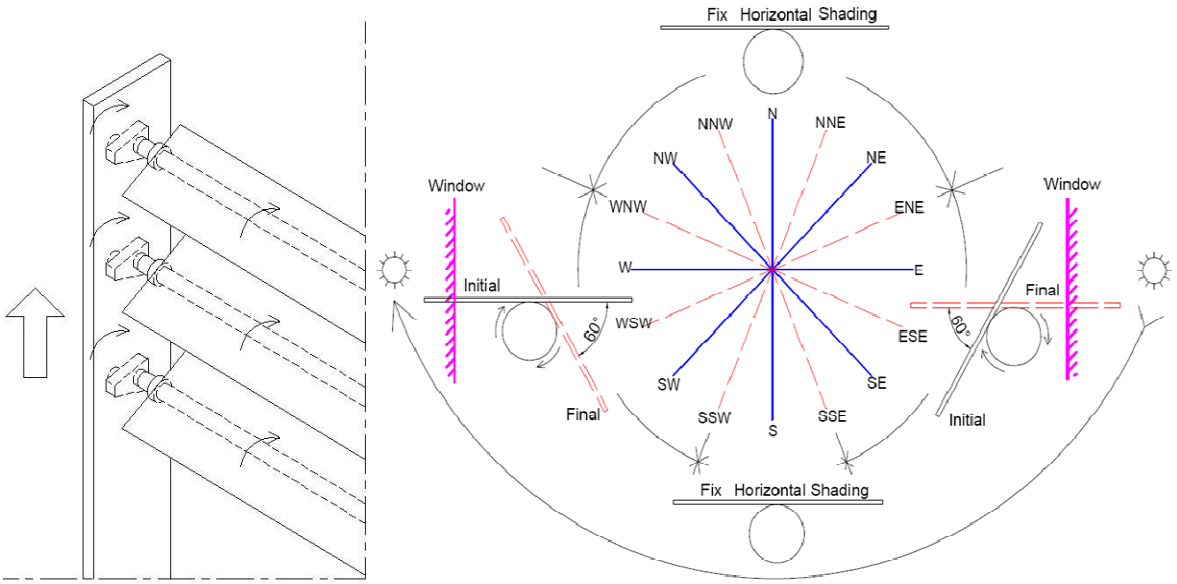

Figure 3. The driving and rotating mechanisms of blinds.

Figure 4. A typical window in Taiwan, with bars to enhance security.

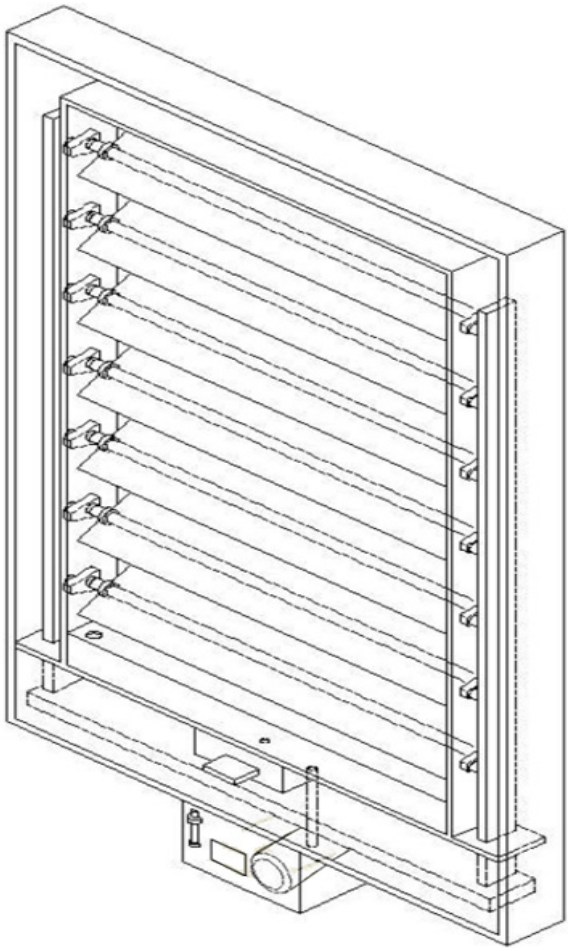

Figure 5. Relief assembly drawing of the shading device.

3.3. Detail Design

The drive device includes a floating board that is installed in the compartment by floating it on the liquid surface. Furthermore, a pair of interlinking components mounted on the floating board is connected to one end of the sun-shading panel in order for the panel to rotate towards the intended direction. The interlinking components include a drive lever, which is connected to the floating board

and is equipped with several pivots. One end is connected to the drive level with he other connected to the sun-shading panel. In the liquid compartment, a flow rate control device is provided (Figure 6a), which is connected to upper and lower chambers. This device operates to guide the liquid from the upper chamber to the lower chamber at the set flow rate (or within the required time). The control device is provided with an inlet that links the upper chamber with the outlet connecting to the lower chamber. On the base, several corresponding drainage holes in varied calibers (Figure 6b) are provided in order to control the flow rate and liquid level rising speeds. The outward pulling or inward pushing forces (aligning with the drainage holes) of motion component in the cutting slot so as to obtain the sun-shielding time desired by the user. The rotation of blind slats is primarily controlled by the buoyancy effect induced by the amount of flow-in liquid, the trigger of the movement could be regulated by the motor from pumping the liquid in the lower chamber to the upper chamber. The liquid will naturally flow down via apertures on the separating board, which is placed between the upper and the lower chamber, to the lower chamber by gravity. The buoyancy function is therefore effected to raise the floating board upward and trigger the movement of the pivot. Consequently, the desired rotation speed could be regulated by subtle adjusting/selecting the apertures with various diameters through the flow rate control device. This design meets the user-friendly design requirement. A motor is installed in the liquid compartment in order to convey the liquid from the lower chamber to the upper one. This allows the liquid to flow downwards and push the floating board toward the sun-shading panel. Through this configuration, automatic operation is possible. The moving status of the floating board is shown in Figure 7. The motor is used to pump the liquid to the upper chamber before use or in the early morning of the following day; the setting varies according to the orientation selected. The volume is controlled by the liquid level controller; this is necessary to generate the liquid volume required to turn the sun-shading panel to 60°.

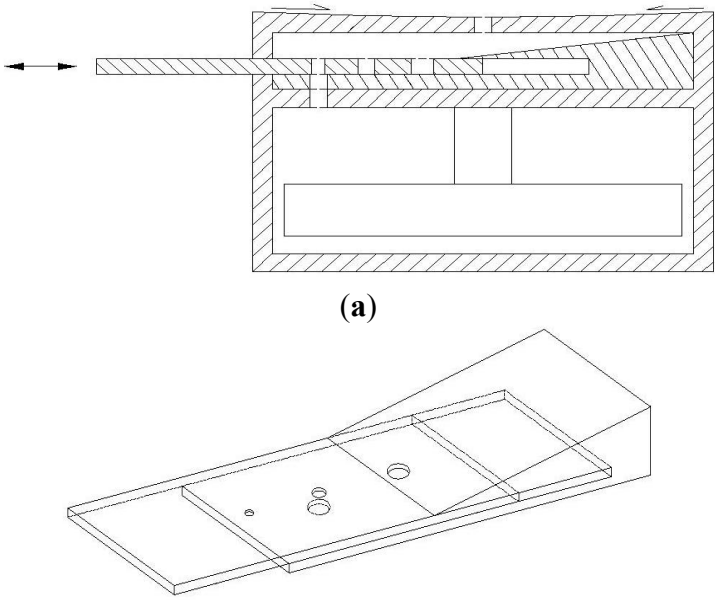

(**a**)

(**b**)

Figure 6. Liquid Compartment: (**a**) Section drawing of the liquid compartment, which indicates the space relationship between control device and upper/lower chambers; (**b**) Flow rate control device.

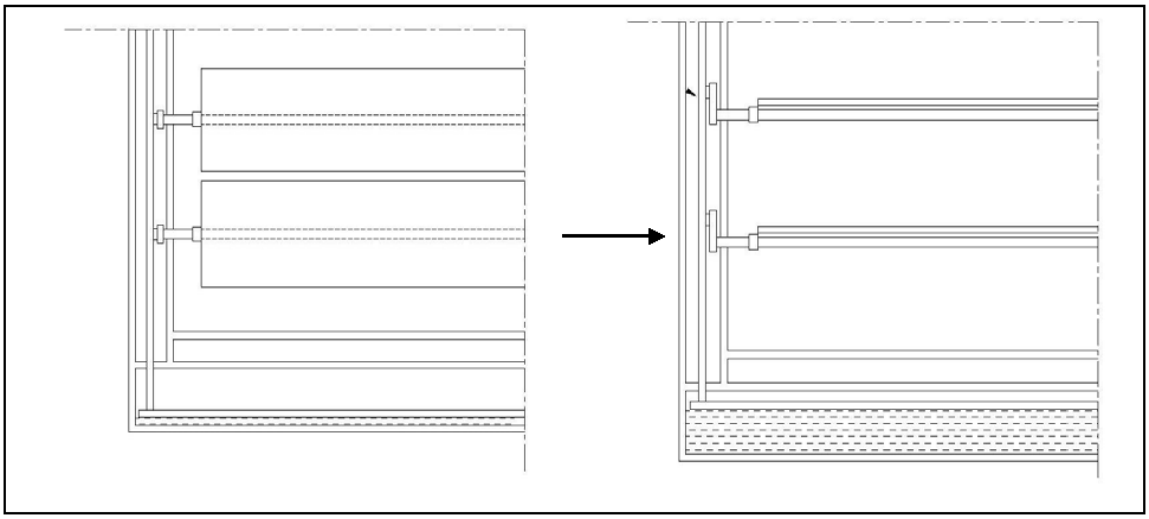

Figure 7. The moving status of floating board.

4. Impact on Indoor Environment

The exterior shading devices are capable of blocking the incoming solar radiation that falls on the fenestration surface, thus reducing the overall solar radiation heat gain. There are two major sun-blocking effects generated by exterior shading devices: (1) reducing the energy consumption of air-conditioning systems; and (2) improving the indoor thermal environment. The cooling energy is saved due to a reduced cooling load resulting from the prevention of excessive indoor solar radiation gain. Moreover, although the indoor environment is air-conditioned, occupants near the window may be vastly influenced by solar radiation and will experience thermal discomfort due to the rising indoor mean radiant temperature (T_{mrt}). This is particularly relevant to spaces with large exterior glass façades. Lower space temperature is required to compensate the rising T_{mrt} in order to achieve thermal comfort. However, the Taiwanese government stipulates that the temperature in air-conditioned public spaces must be held constantly at 28 °C, for the purposes of energy conservation. The radiant effect from the windows may severely impact the thermal comfort environment. Using exterior blinds as a sunshade is a strategy that can lower the indoor heat stress caused by the radiation effect. The analyses of these two effects are discussed below.

4.1. Simulation Tools

To understand the effects of the automatic blind device, we simulated a typical office space using EnergyPlus, which is a building energy analysis and thermal load simulation program developed by the U.S. Department of Energy. It was developed based on a heat balance method and was tested against ASHRAE Standard 140 [23]. Henninger *et al.* also validated the program using a test suite of 14 building cases which included varying internal loads and outdoor conditions, and revealed that EnergyPlus agreed well with other building simulation programs [24]. For more details in regard to the energy and daylighting calculation algorithms the reader may refer to [25]. This program has already been widely adopted in simulating the exterior blind system to derive its energy or thermal performance [26–28]. Furthermore, some studies have successfully utilized this software for daylighting analysis [29–31].

4.2. Description of the Design of a Typical Office Simulation Model

The geometry of the typical office, the construction properties, and the related simulation parameters are tabulated in Table 2. The model is illustrated in Figure 8. The office is a single-sided exterior space with an 80% window-to-wall ratio, located on the middle floor of a mid-rise building. The effectiveness of cooling energy savings and thermal comfort enhancement were compared to a case study without exterior blinds. Through careful adjustment of the amount of water being pumped into the window frame, the rotation speed of each blind slat can be regulated at a constant speed. In the simulation cases, we assumed that the blind slats rotate from horizontal to vertical positions every 6 h during the occupied hours, *i.e.*, the blind is completely open at 6:00 and completely closed at 12:00, and returns to being open at 18:00, and so on. These rotations are necessary in order to control the solar insulation effect through the window. The blind system fully covers the front of the model's fenestration area and is equal to an area of 14.4 m^2. The width of each blind slat is 30 cm and the vertical distance between every pair of slats is 30 cm. The distance between the plumb line of the exterior blind system's rotating axes to the window glass façade is 20 cm, which is partitioned just enough to allow the blind slats to rotate. In order to understand the effect of blinds in every facing direction, the exterior facade of the model was adjusted to eight orientations during each case simulation, and each orientation simulation result was compared to the same corresponding orientation case without blinds. The hourly local meteorological years (TMY3) of Taipei and Kaohsiung were used for the simulation instead of using a certain year's weather data to obtain climatically representative results. The climate of the chosen cities distinctly represent two major climate zones in Taiwan, which according to Köppen-Geiger's climate classification system [32] the northern Taipei (25.04 N, 121.51 E) is of Cfa (hot-and-humid) climate and the southern Kaohsiung (22.57 N, 120.31 E) is of Cwa (hot-and-humid summer with dry winter) climate. The climatic conditions of the two cities are shown in Figure 9. The monthly average dry-bulb temperatures are 23.3 °C and 25.5 °C for Taipei and Kaohsiung respectively. The annual cooling degree day calculated based on 18 °C in turn are 2139 K.h and 2768 K.h. The running period of the simulation covers one full year and is carried out on an hourly basis. The output of each simulation included: hourly sensible cooling loads, hourly ambient temperature, mean radiant temperature and solar radiation heat gain of the interior.

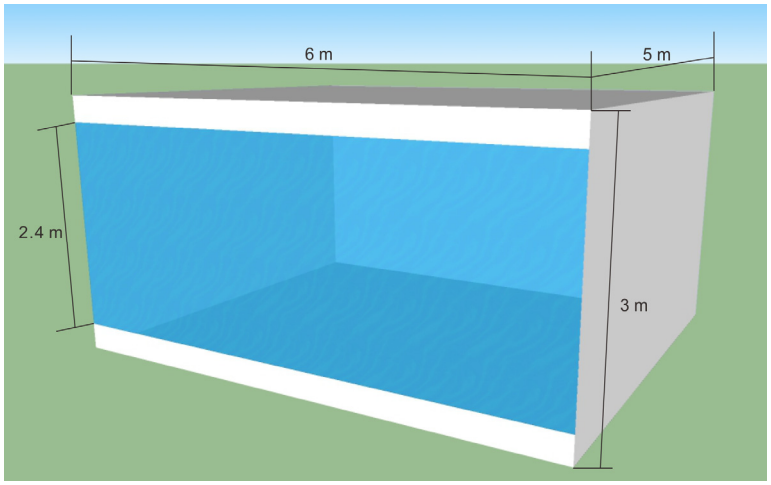

Figure 8. Model of typical glass curtain wall office space for simulation.

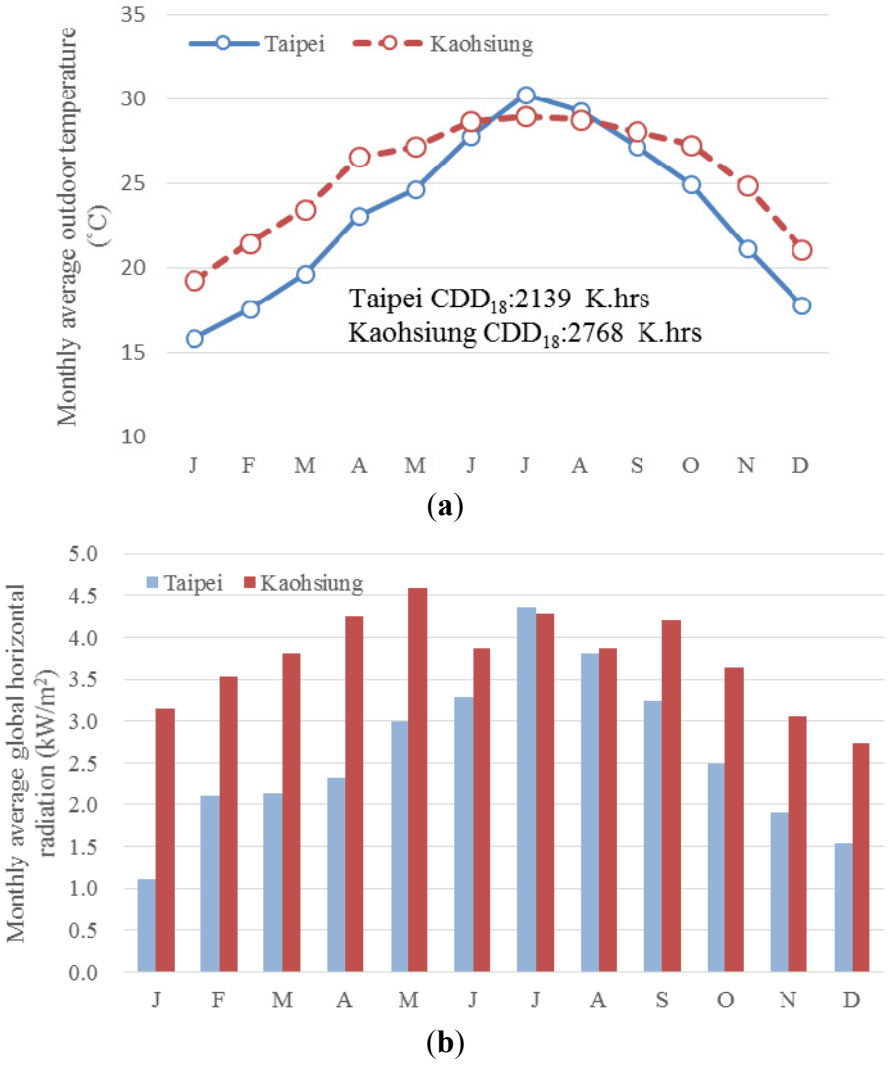

Figure 9. Climatic conditions of Taipei and Kaohsiung (**a**) outdoor temperature with annual cooling degree days (**b**) global solar radiation.

Table 2. Description of the simulated space.

Item	Description
Space geometry	Width = 6.0 m; Depth = 5.0 m; Ceiling height = 3.0 m; with one 6.0 m exterior exposed wall
Exterior wall construction	Construction from outside layer to inside layer: 30 mm marble, 30 mm mortar, 150 mm reinforced concrete, 10 mm cement fiber board; equivalent to U-value = 2.76 W/(m^{2}K)
Windows	Window-to-wall ratio = 80%; Window width = 6.0 m; Window height = 2.4 m
Window glass	6 mm Clear glass; U-value = 5.78 W/(m^{2}K); SHGC [1] = 0.82
Blinds	Thickness = 0.25 mm; Blind slat width = 300 mm; Slat separation distance = 300 mm; Conductivity = 211 W/(mK); Slat surface reflectance = 0.7
Blind rotation mechanism	East: 0° (horizontal) to 60° from 06:00 to 12:00 and is fixed at 0° for the other hours. West: 0° (horizontal) to 60° from 12:00 to 18:00 and is fixed at 0° for the other hours. North and South: All day fixed at 0°.
Internal heat gain	Occupancy density = 0.2 person/m^2; Lighting density = 15W/m^2; Appliances power density = 10 W/m^2; Weekday's occupied hours = 08:00–17:00
HVAC system	VAV system with chiller capacity of 3.93 kW, Nominal COP = 6.5; Economizer = none; Cooling setpoint = 24 °C (winter) & 28 °C (summer); Outside air flow rate = 9.4 L/s per person; Cooling hours: 08:00–17:00

[1] SHGC denotes to solar heat gain coefficient of the window glass.

4.3. Impact on Energy Performance Results

The impacts of blinds on energy performance was discussed in two ways: the reduction rate of solar radiation and the sensible cooling energy savings. From Figure 10 it can be seen that the blind system could stop most direct solar radiation from transmitting to indoors, but the amount of the reduction would highly depend on the facing orientation of the windows. The amount of annually reduced direct solar radiation is largest in the SE and SW orientations, a reduction of 1,483 kWh and 1,127 kWh, corresponding to 56% and 49% reduction rates, respectively. Although the reduction rates for NE and NW orientation cases were high, the amount of direct solar radiation reduced was limited. The reduction rates for the diffuse solar radiation were similar for all orientations. It is worth mentioning that although the amount of diffuse radiation is larger than the direct radiation, its contributions to the cooling energy and the indoor thermal condition are different. The cooling energy is much more sensitive to direct solar radiation than to diffuse solar radiation. To understand this effect, sensible cooling loads for each orientation were analyzed in two climatic zones. Taipei city is located in northern Taiwan and experienced a hot-and-humid subtropical climate. On the other hand, Kaohsiung city is located in southern Taiwan, with a very hot-and-humid tropical climate.

From the results depicted in Figure 11, the cooling energy saving in Kaohsiung peaked in the SW orientation with a 30.2% saving ratio followed by the SE, W, E, S, NW, NE, and N orientations. The results from Taipei are slightly different, the cooling energy saving peaked in the SE orientation with 28.9% saving ratio followed by the E, SW, W, S, NE, NW, and N orientations. The evidence suggests that the cooling energy saving is larger in the east in northern Taiwan and in the west and south side in southern Taiwan. Based on the discrepancies observed between the two cities, we can speculate that the probability of rain in the afternoon is higher in Taipei than in Kaohsiung. This results in a larger cooling demand in the morning, when the sun is in the east, than in the afternoon. Figure 12 illustrates the simulation results of hourly variations of sensible cooling energy and the transmitted total solar radiation over two consecutive typical sunny summer days in Taipei. Since the solar radiation is effectively blocked by the blind system, the cooling energy is drastically reduced over time.

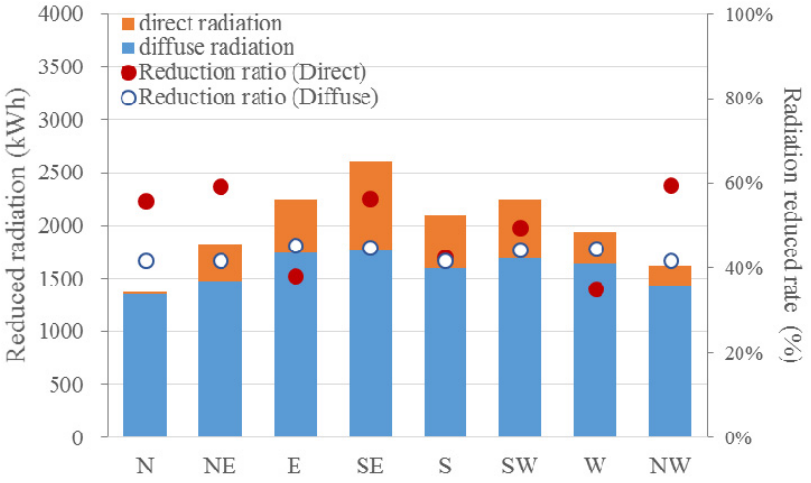

Figure 10. Annual total reduced solar radiation in various facing orientation with blinds.

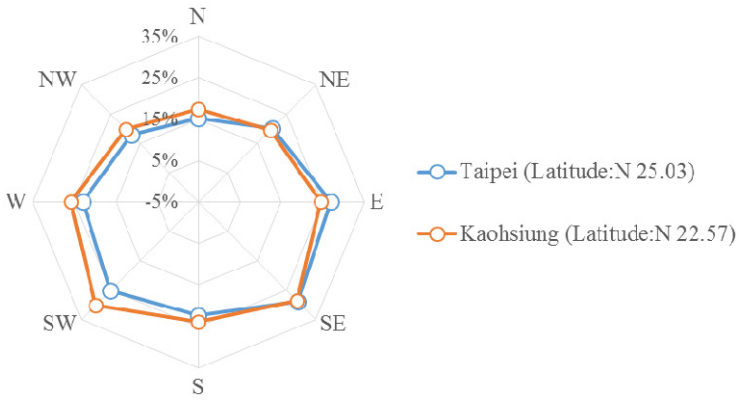

Figure 11. Cooling energy saving rate of every direction.

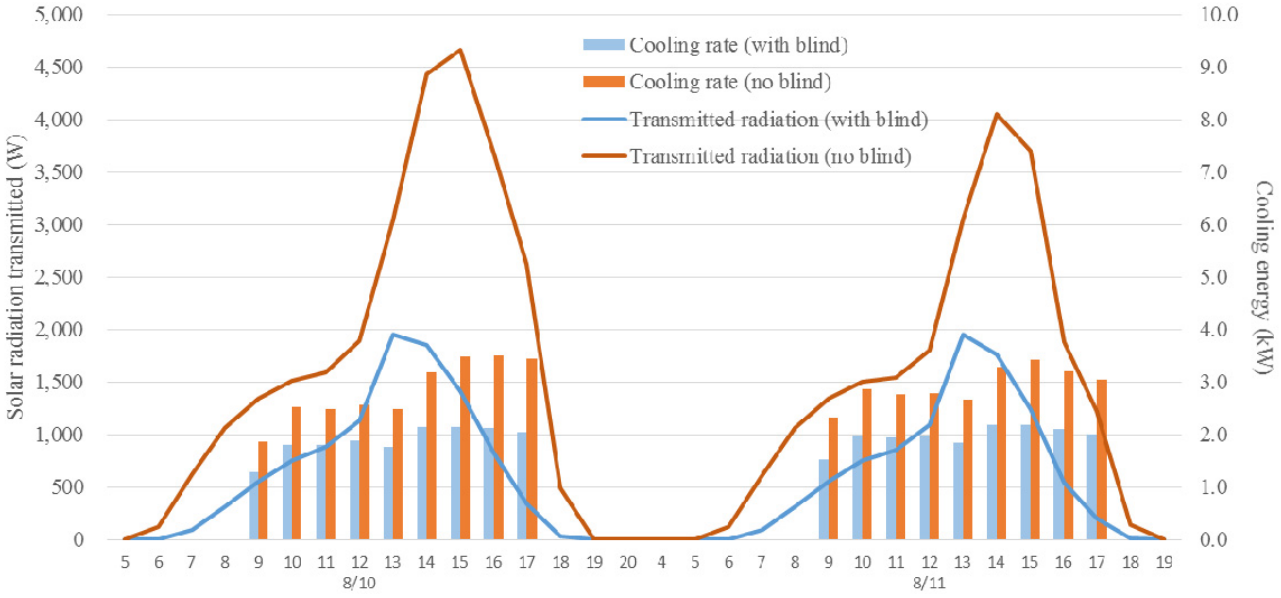

Figure 12. Hourly solar radiation transmitted into indoors and the corresponding cooling energy rates on two typical consecutive summer days in Taipei.

4.4. Impact on Indoor Thermal Comfort Results

In order to study the indoor thermal condition change after applying an exterior blind system in an air-conditioned room, an adaptive thermal comfort evaluation was performed. The adaptive thermal comfort model hypothesizes that occupants' perceptions of thermal comfort are adaptive to the outdoor environment when occupants have control over either mechanical or passive thermal regulating means. The adaptive model used here is proposed by the ASHRAE standard 55 [33]. The thermal comfort neutral operative temperature (T_c) is a function of outdoor monthly running mean temperature (T_{rm}), as Equation (1). The acceptable upper/lower temperature limits are ±3.5 °C higher/lower than the T_c. Any indoor operative temperature (T_{ot}), which reflects both radiant and temperature effect on thermal comfort and can be estimated via Equation (2), outside this range is considered to represent thermal discomfort.

To describe the thermal discomfort condition of the indoor thermal environment from long-term (yearly) perspective, two indices suggested by ISO 7730 [34] were used, the discomfort occurrence

frequency and the discomfort severity. Both are evaluated hourly whenever the space is occupied. As the frequency of discomfort alone only delivers the information of the discomfort occurrence probability, the severity of overheating or overcooling remains unknown. The long-term severities of thermal discomfort (*I*) for evaluating long-term discomfort severity was therefore introduced. The frequencies of indoor discomfort (ξ) during occupied hours can be estimated from a series of hourly indoor operative temperatures predicted through simulation. Moreover, the long-term severities of thermal discomfort (*I*), either overheating or overcooling, were assessed through the weighted degree-hour method, which is cumulated over one year period. The calculation of *I* index with a weighting factor (*wf*), which deems discomfort to be proportional to the degree by which the discomfort threshold is exceeded by the upper/lower limit of the thermal comfort range, is as Equation (3). When the hourly indoor T_{ot} falls beyond the lower or upper limit ($T_{c,limit}$) of the adaptive thermal comfort range suggested by ASHRAE Standard 55, the difference is measured, and a weighting factor is applied to quantify the severity of thermal discomfort of that particular hour. The warm and cold period severity of long-term discomfort (I_{warm} and I_{cold}) are therefore estimated via Equations (4) and (5):

$$T_c = 0.31 \times T_{rm} + 17.6 \tag{1}$$

$$T_{ot} = 0.5 \cdot (T_a + T_{mrt}) \text{ for } v < 0.2 \text{ m/s} \tag{2}$$

$$wf = 1 + \frac{\left|T_{ot} - T_{c,limit}\right|}{\left|T_c - T_{c,limit}\right|} \tag{3}$$

$$I_{warm} = \sum wf \cdot t \text{ for } T_{ot} > T_{c,limit} \tag{4}$$

$$I_{cold} = \sum wf \cdot t \text{ for } T_{ot} < T_{c,limit} \tag{5}$$

where *wf* is the weighted factor; T_{ot} is an hourly indoor operative temperature; the $T_{c,limit}$ is the upper or lower limit of the thermal comfort range; *t* is time span, which is 1.0 hour in this study; *v* is indoor wind velocity.

The evaluation results in Figure 13 and Table 3 reveal that the overheating occurrences and the overheating severities are due to excessive radiant heat gain in an air-conditioned environment with or without utilizing the blind system. In the warm season, from July to October for instance, the case without blinds experienced high frequencies as well as high severities of overheating, especially in Kaohsiung. As illustrated in Figure 13, the monthly mean indoor operative temperatures for the case without blinds were over the upper thermal comfort limit from May to November. In contrast, in the case with blinds, the monthly mean of operative temperatures of all the months was within the limit. This suggests that the blind system is effectively enhancing the indoor thermal comfort of the space. The blind system is capable of reducing the overheating risk for both cases in Taipei and Kaohsiung. The values of the effectiveness ratio of blinds, defined as the reduction rate of certain variables, either the frequency or severity are both larger in Taipei than in Kaohsiung. In contrast, as cooling demand is much higher in Kaohsiung, the reduction ratio of cooling energy is larger compared to that of Taipei, which is 32.8% and 27.9%, respectively. Furthermore, because of the poor thermal insulation property of glass curtain wall, indoor radiant cooling may occur resulting in overcooling discomfort occurrences in winter. The case with blinds was able to reduce both the overcooling occurrence frequency and its

severity, through reducing the radiant cooling process. Moreover, to further compare the proposed buoyancy-driven dynamic blind system with widely used traditional exterior venetian blind systems with fixed horizontal slats, simulations were performed for traditional fixed blinds with the same physical slat properties as the proposed one. The results are listed in the rightmost column in Table 3. The proposed buoyancy-driven dynamic blind system could further improve the indoor comfort condition by reducing the overheating occurrence frequency and the overheating severity by 5.7% and 7.5% respectively in Taipei, and 3.5% and 7.9% in Kaohsiung. The annual cooling energy could also be reduced by a further 5.8% and 8.2% for Taipei and Kaohsiung respectively.

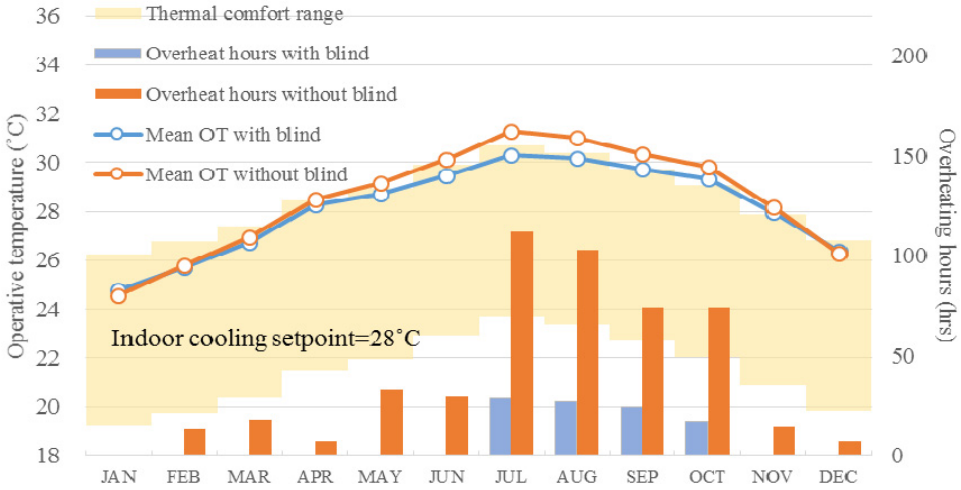

Fugure 13. Monthly mean indoor operative temperature (T_{ot}) and monthly number of overheating hours under constant 28 °C cooling setpoint during space occupied hours (SW, Taipei case).

4.5. Effectiveness of the Blind System with Various Thermal Properties of Glazing

The previous sections evaluated and discussed the effectiveness of the blind system applied in buildings with 6 mm glazing (SHGC = 0.82 and U-value = 5.78), which is the most commonly seen in the Taiwanese building industry. As the effectiveness could be dependent to the thermal properties of building façade, a sensitivity study of the effectiveness against thermal properties of glazing was performed. The same building model was used for simulation except for the changing of glazing's solar transmittance property (SHGC) and insulation property (U-value). Three new models with combinations of their glazing with lower SHGC and U-value were generated. The simulations of SW oriented facade were performed with Taipei's TMY3.

Table 3. Thermal comfort alleviating and sensible cooling energy saving potential of blinds in Taipei and Kaohsiung for SW oriented case.

Location	Comparison Items		Reduction Ratio of the Proposed Blind As Compared to the Case Without Blind	Reduction Ratio of the Proposed Blind As Compared to Traditional Fixed Blind
Taipei *[1]	Overheating	frequency, ξ (h)	24.5%	5.7%
		severity, *I* (K·h)	31.1%	7.5%
	Overcooling	frequency, ξ (h)	55.3% *[3]	10.5% *[3]
		severity, *I* (K·h)	53.1% *[3]	9.6% *[3]
	Sensible cooling energy (kWh)		27.9%	5.8%
	Orientation sensitivity order for energy saving		SE > E > SW > W > S > NE > NW > N	
Kaohsiung *[2]	Overheating	frequency, ξ (h)	11.9%	3.5%
		severity, *I* (K·h)	25.4%	7.9%
	Overcooling	frequency, ξ (h)	N/A *[4]	N/A *[4]
		severity, *I* (K·h)	N/A *[4]	N/A *[4]
	Sensible cooling energy (kWh)		32.8%	8.2%
	Orientation sensitivity order for energy saving		SW > SE > W > E > S > NW > NE > N	

*[1] Hot-and-humid climate; *[2] Hot-and-humid summer with dry winter climate; *[3] The number of overcooling occurrence hours for these comparison are all less than 50 h annually, which compares to those of overheating problem (usually larger than 1000 h) is much less; *[4] There are no overcooling problem for the case in Kaohsiung.

The effectiveness of the blind system is defined as the annual indoor thermal overheating alleviation ratio or annual cooling energy reduction ratio in comparison with the base case without the exterior blind applied. In order to identify how different glazing thermal properties would affect the effectiveness of the blind system, each value of the effectiveness shown in Table 4 was calculated with respect to their corresponding base case having the same SHGC and U-value. As can be seen in Table 4, effectiveness with respect to both overheating frequency and severity doesn't change much. The effectiveness on indoor thermal comfort generally slightly decreases either for cases with improved SHGC or U-value. In contrast, the effectiveness on annual energy conservation decreases for the case with improved SHGC, but increases for the case with improved U-value. It suggests that cooling energy is more sensitive to heat gains from solar radiation than from heat transfer. Since the glazing with improved SHGC have offered better solar radiation blocking ability, the effectiveness of the blind system, which literally provides the same solar radiation blocking effect as SHGC, on cooling energy is therefore reduced.

Table 4. The effectiveness matrix of the blind with various combination of SHGCs and U-values of the glazing.

SHGC	U-Value					
	5.78 (W/m^2)			4.4 (W/m^2)		
	Overheating Frequency	Overheating Severity	Cooling Energy	Overheating Frequency	Overheating Severity	Cooling Energy
0.82	24.5% (−)	31.1% (−)	27.9% (−)	21.6% (−2.9%)	29.6% (−1.5%)	29.4% (+1.5%)
0.5	22.6% (−1.9%)	27.6% (−3.5%)	20.8% (−7.1%)	24.6% (+0.1%)	30.0% (−1.1%)	23.1% (−4.8%)

4.6. Daylighting Performance Analysis

Daylighting performance and visual comfort of the proposed blind system application were analyzed against cases of fixed blind and without blind. Hourly spatial metrics of indoor daylighting illuminances and glare probabilities were simulated and outputted via EnergyPlus with Taipei's TMY3. A dynamic daylighting performance metric, *i.e.*, useful daylight illuminance (UDI), was used to characterize the effective daylighting both temporally and spatially. UDI measures the daylight illuminance between 100 and 2000 lux as effective/useful daylighting and counts the annually proportion of the number of hours/points falling within the range during the occupied hours. The results were tabulated in Table 5, where it can be seen that the proposed blind system is able to improve the annual UDI by 13.2% to 23.8% among various orientations, having laterally the same effect as the fixed blind. It is speculated that the blind system is able to reduce the excessive amount of daylight illuminance and lower the probability of over illuminating, resulting in better illuminating environment than the cases without blinds. The temporally mapped UDI distribution across one year of a west facing case was plotted in Figure 14.

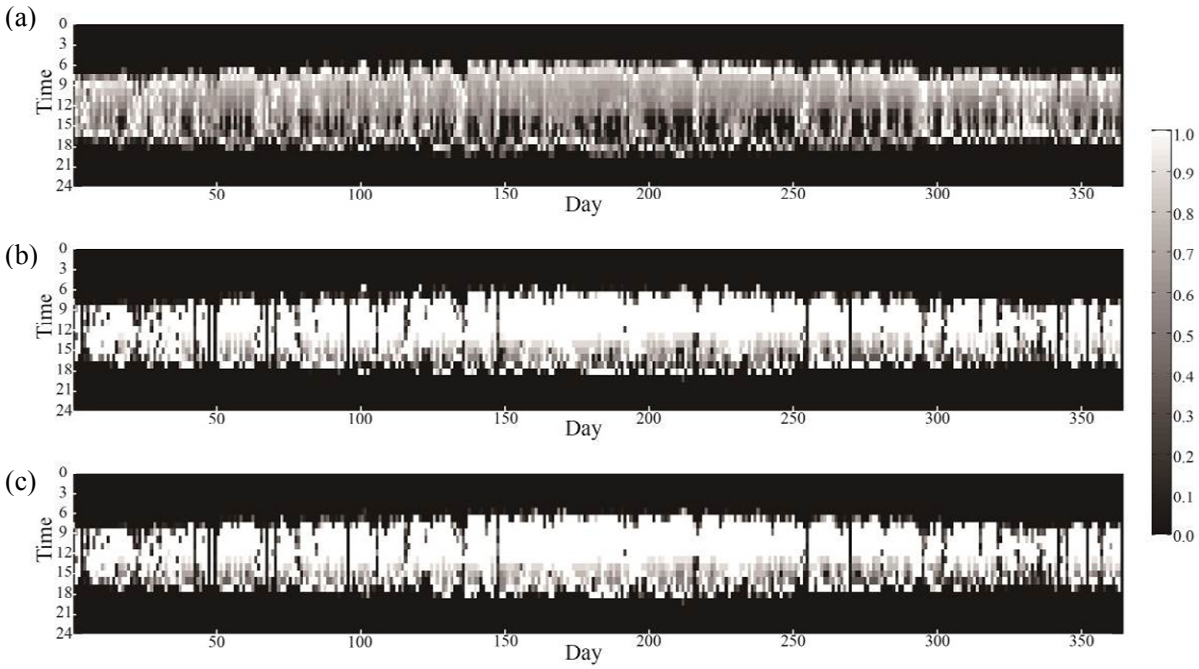

Figure 14. Temporal distribution map of UDI for the west facing case. (**a**) Without blind; (**b**) with fixed blind; (**c**) with the proposed blind.

Table 5. Annual UDI and occurrence probability of disturbing/intolerable glare during occupied hours (DGI > 24).

Orientation	$UDI_{100\text{-}2000\ lux}$			DGI > 24		
	No Blind	Fixed Blind	Proposed Blind	No Blind	Fixed Blind	Proposed Blind
N	67.8%	80.9%	80.9%	53.3%	0.0%	0.0%
E	61.2%	77.9%	77.9%	58.9%	19.9%	19.6%
S	53.0%	76.7%	76.7%	59.3%	8.3%	8.3%
W	55.7%	76.9%	77.1%	56.3%	11.0%	10.5%

1. Daylight glare index (DGI) was adopted to analyze the glare problem to address the visual comfort issue. The calculation of DGI is as Equation (6). Jakubiec and Reinhart suggested four levels of the degree of perceived glare and considered it intolerable when DGI > 31 and imperceptible when DGI < 18 [35]. Figure 15 illustrates the annual temporal distribution of the DGI categorized according to the four levels of a west facing space. From Figure 15 and Table 5, the blind system, either fixed or the proposed one, are capable of efficiently alleviating the glare problem and enhancing the visual comfort, regardless of orientation.

$$DGI = 10 \cdot \log\left(0.478 \sum_i \frac{L_{s,i}^{1.6} \cdot \omega_{s,i}^{0.8}}{L_b + 0.07\omega_{s,i}^{0.5} \cdot L_{s,i}}\right) \quad (6)$$

where L_b is background luminance (cd/m^2); $L_{s,i}$ is the luminance of the glare source i (cd/m^2); $\omega_{s,i}$ is the solid angle of source i (sr).

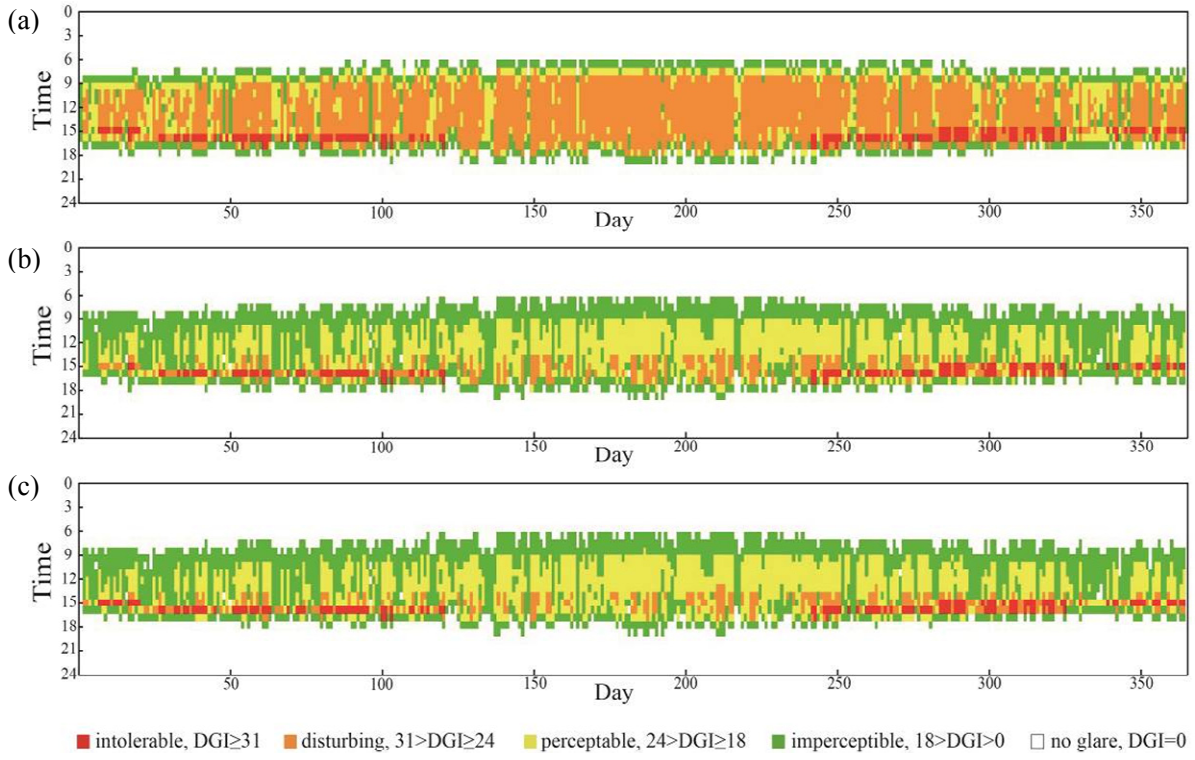

Figure 15. Temporal distribution map of DGI for the west facing case. (**a**) Without blind; (**b**) with fixed blind; (**c**) with the proposed blind.

5. Conclusions

The purpose of this paper was to propose a design for an external shading device in order to effectively control the indoor environment. A simulation analysis of a typical office space is conducted in order to understand the impacts of the external shading devices on energy performance and indoor thermal comfort. The innovation of the blind system proposed is described below. Traditional manually operable shading devices, although energy free while in operation, in actual utilization they were not that satisfactory in regards to achieving the maximum benefits between the trade-off in energy performance and daylighting availability due to the fact of tremendous uncertainties of human behaviors. Conversely, an automatic adjustable shading device could easily overcome the above problem by introducing logistic control but consumes a lot of electricity because the motorized mechanical system needs to continually commence the rotation of the blind slats. The solution provided herein would balance the inefficiency usage of the exterior blind and the energy consumption of the blind system. Furthermore, this system could be customized to respond to the daylighting and energy conservation needs with maximum results without using much electricity as compared to the other automated blind systems. We offer a possible alternative option for the choice of exterior shading system. The main application of the shading devices would be for the office spaces or houses with excessive solar heat gain that also have daylighting demands simultaneously. One potential future research direction would be the bi-objective optimization problem between energy saving and visual comfort by adjusting the movement of blind slats. Through the design methodology and the simulation results, some overall conclusions were derived:

(1) In this paper the design considerations, design concept, and detailed design of the automatic buoyancy-shading device for building applications was presented. The choice of materials for the design creates the extra function, as discussed in above sections. The automatic shading device is unique in its driving and control mechanisms, it can be easily used and set up on typical windows in Taiwan.
(2) Controllers for the panel positioning are often very complex and confusing. However, our design seems to satisfy user preferences and is convenient to use.
(3) It is possible to improve user expectations and replace conventional shading devices with simplified and effective designs.
(4) The effectiveness of the blind system was evaluated with regard to the improvement of indoor thermal comfort and the cooling energy saving. The results revealed that there was a 24.5% and 11.9% reduction in the occurrence of overheating when using the automated blind for the SW case in Taipei and Kaohsiung, respectively. The overheating severity alleviated by the blinds could also reach 31.1% and 25.4%, suggesting that blinds are a promising method for improving indoor thermal comfort.
(5) The cooling energy saving potential was 27.9% and 32.8% for Taipei and Kaohsiung, respectively. This reveals that in a centrally air-conditioned space, there is efficient energy saving potential.
(6) The cooling energy saving effectiveness of the blind system would decrease with the improvement of glazing's solar radiation blocking ability (*i.e.*, SHGC), but would increase with the improved glazing insulation property (*i.e.*, U-value).
(7) The proposed blind system is capable of both improving the usage of daylighting and also reducing the glare problem.

Acknowledgments

Thanks to the Alumni Association of National United University for financial support for this design.

Author Contributions

Han-Hsi Liang was responsible for the overall coordination of the research team and developed the design mechanism of the blind system and thermal comfort analysis. Kuo-Tsang Huang did the energy, thermal comfort and daylighting simulations and interpreted the results. Kevin Fong-Rey Liu did the literature review and help collect the data. All authors were involved in discussing the research and have read as well as approved the manuscript.

Conflicts of Interest

The authors declare no conflict of interest.

References

1. Chen, H.J.; Wang, D.W.P.; Chen, S.L. Optimization of an ice-storage air conditioning system using dynamic programming method. *Appl. Therm. Eng.* **2005**, *25*, 461–472.

2. Yang, K.H.; Hwang, R.L. Energy conservation of building in Taiwan. *Pattern Recogn.* **1995**, *28*, 1483–1491.
3. Kim, G.; Lim, H.S.; Lim, T.S.; Schaefer, L.; Kim, J.T. Comparative advantage of an exterior shading device in thermal performance for residential buildings. *Energy Build.* **2012**, *46*, 105–111.
4. Adriaenssens, S.; Rhode-Barbarigos, L.; Kilian, A.; Baverel, O.; Charpentier, V.; Horner, M.; Buzatu, D. Dialectic form finding of passive and adaptive shading enclosures. *Energies* **2014**, *7*, 5201–5220.
5. Yener, A.K. A method of obtaining visual comfort using fixed shading devices in rooms. *Build. Environ.* **1998**, *34*, 285–291.
6. Carbonari, A.; Rossi, G.; Romagnoni, P. Optimal orientation and automatic control of external shading devices in office buildings. *Environ. Manag. Health* **2002**, *13*, 392–404.
7. Datta, G. Effect of fixed horizontal louver shading devices on thermal perfomance of building by TRNSYS simulation. *Renew. Energ.* **2001**, *23*, 497–507.
8. Manzan, M.; Padovan, R.; Clarich, A.; Rizzian, L. Energy and daylighting optimization for an office with fixed and moveable shading devices. In Proceedings of the 2014 Building Simulation and Optimization Conference, London, UK, 23–24 June 2014.
9. Hammad, F.; Abu-Hijleh, B. The energy savings potential of using dynamic external louvers in an office building. *Energy Build.* **2010**, *42*, 1888–1895.
10. Nielsen, M.V.; Svendsen, S.; Jensen, L.B. Quantifying the potential of automated dynamic solar shading in office buildings through integrated simulations of energy and daylight. *Solar Energy* **2011**, *85*, 757–768.
11. Atzeri, A.; Cappelletti, F.; Gasparella, A. Internal *versus* external shading devices performance in office buildings. *Energy Procedia* **2014**, *45*, 463–472.
12. Guillemin, A.; Molteni, S. An energy-efficient controller for shading devices self-adapting to the user wishes. *Build. Environ.* **2002**, *37*, 1091–1097.
13. Gugliermetti, F.; Bisegna, F. Daylighting with external shading devices: Design and simulation algorithms. *Build. Environ.* **2006**, *41*, 136–149.
14. Manzan, M. Genetic optimization of external fixed shading devices. *Energy Build.* **2014**, *72*, 431–440.
15. Tumer, J.S. *Buoyancy Effects in Fluids*; Cambridge University Press: New York, NY, USA, 1979.
16. Royden, L.H.; Husson, L. Subduction with variations in slab buoyancy: Models and application to the banda and apennine systems. In *Subduction Zone Geodynamics, Frontiers in Earth Sciences*; Springer: Berlin, Germany, 2009; pp. 35–45.
17. Spaeth, M.; Barthlott, W. Lotus-effect (R): Biomimetic super-hydrophobic surfaces and their application. *Smart Textiles* **2009**, *60*, 38–46.
18. Prasad, C.V.; Rao, K.C.; Reddy, G.V.; Rani, T.S.; Yerriswamy, B.; Subha, M.C.S. Characteristic studies of ligno-cellulosic fabric grewia tenax. *J. Nat. Fibers* **2010**, *7*, 194–215.
19. Cheng, C.L.; Liao, L.M.; Chou, C.P. A study of summarized correlation with shading performance for horizontal shading devices in Taiwan. *Sol. Energy* **2013**, *90*, 1–16.
20. Pacheco, R.; Ordóñez, J.; Martínez, G. Energy efficient design of building: A review. *Renew. Sustain. Energy Rev.* **2012**, *16*, 3559–3573.

21. Cho, J.; Yoo, C.; Kim, Y. Viability of exterior shading devices for high-rise residential buildings: Case study for cooling energy saving and economic feasibility analysis. *Energy Build.* **2014**, *82*, 771–785.
22. Birnbaum, L.; Lieberman, H.; Horvitz, E.; Marks, J.; Kurlander, D.; Roth, S. Compelling intelligent user interfaces—How much AI. In Proceedings of the 1997 International Conference on Intelligent User Interfaces, New York, NY, USA, 6–9 January 1997.
23. ANSI/ASHRAE Standard 140. *Standard Method of Test for the Evaluation of Building Energy Analysis Computer Programs*; American Society of Heating, Refrigerating and Air Conditioning Engineers: Atlanta, GA, USA, 2011.
24. Henninger, R.H.; Witte, M.J.; Crawley, D.B. Analytical and comparative testing of EnergyPlus using lEA HVAC BESTEST E100-E200 test suite. *Energy Build.* **2004**, *36*, 855–863.
25. Lawrence Berkeley National Laboratory (LBNL). *EnergyPlus Engineering Reference-The Reference for EnergyPlus Calculations*; LBNL: Berkeley, LA, USA, 2007.
26. Carletti, C.; Sciurpi, F.; Pierangioli, L. The energy upgrading of existing buildings: Window and shading device typologies for energy efficiency refurbishment. *Sustainability* **2014**, *6*, 5354–5377.
27. Shen, E.; Hu, J.; Patel, M. Energy and visual comfort analysis of lighting and daylight control strategies. *Build. Environ.* **2014**, *78*, 155–170.
28. Kim, D.W.; Park, C.S. Comparative control strategies of exterior and interior blind systems. *Lighting Res. Technol.* **2012**, *44*, 291–308.
29. Li, D.H.W.; Wong, S.L. Daylighting and energy implications due to shading effects from nearby buildings. *Appl. Energy* **2007**, *84*, 1199–1209.
30. Mettanant, V.; Chaiwiwatworakul, P. Automated vertical blinds for daylighting in tropical region. *Energy Procedia* **2014**, *52*, 278–286.
31. Seo, D.; Ihm, P.; Krarti, M. Development of an optimal daylighting controller. *Build. Environ.* **2011**, *46*, 1011–1022.
32. Kottek, M.; Grieser, J.; Beck, C.; Rudolf, B.; Rubel, F. World Map of the Köppen-Geiger climate classification updated. *Meteorol. Z.* **2006**, *15*, 259–263.
33. ANSI/ASHRAE Standard 55. *Thermal Environmental Conditions for Human Occupancy*; American Society of Heating, Refrigerating and Air-Conditioning Engineers: Atlanta, GA, USA, 2010.
34. ISO Standard 7730. Ergonomics of the thermal environment—Analytical determination and interpretation of thermal comfort using calculation of the PMV and PPD indices and local thermal comfort criteria. International Organization for Standardization: Geneva, Switzerland, 2005.
35. Jakubiec, J.; Reinhart, C. The "adaptive zone"—A concept for assessing discomfort glare throughout daylit spaces. *Light. Res. Technol.* **2012**, *44*, 149–170.